Computer Simulation of Fibre Suspension Flow through a Periodically Constricted Tube

S. B. Shah,
Department of Mathematics,
Shah Abdul Latif University, Khairpur Mirs,
Sindh, Pakistan.
E-mail: baqir.shah@salu.edu.pk

H. Shaikh,
Department of Basic Sciences and Related Studies,
Mehran University of Engineering and Technology,
Jamshoro, Sindh, Pakistan.
E-mail: hisam.shaikh@salu.edu.pk

M. A. Solagni and A. Baloch,
Department of Computer Science,
ISRA University, Hyderabad, Sindh, Pakistan.
E-mail: manwarsolangi@yahoo.com, csbaloch@yahoo.com

Abstract: Present research work focus on a flow of fibres suspended in a Newtonian solvent through periodically constricted tube using a time marching finite element method. A semi implicit algorithm, so called, Taylor Galerken/pressure correction scheme is employed to seek the steady state numerical predictions. Effects of inertia and impact of undulation on flow structure and friction factor is investigated. Co linear fibre constitutive model is adopted along with quadratic closure approximation. Numerical solutions for pure Newtonian fluid are compared and close agreement is realized against experimental as well as numerical results.

AMS (MOS) Subject Classification Codes:
Key Words: Finite Element Method, Newtonian Fluids, Fibre Suspension, Quadratic Closure Approximation and Periodically Constricted Tube.

1. INTRODUCTION

Flow of fibre suspension has great importance in the processing of composite materials, for example (glass, plastic, natural materials, polyethylene, polymer, rigid rod like fibres, food fibres, blood flow in vessels, wood fibres and etc.). The numerical investigation of these flows has attracted number of researchers. Initially, the approach of creeping motion of a single ellipsoid rigid fibre suspended in a Newtonian solvent under simple shear flow as suggested in [1] and was further carried out and extensively studied in [2, 3 and 4]. They derived quadratic closure approximations, for simple shear flow and biaxial elongational

flow, and included the Fockker Plank equation. Whilst, [5] presented a solution technique for long cylindrical rod like fibre that eliminated the need of Fockker Plank equation for the particle orientation distribution functions and reduced the complex computations. Further, the fibre ratios and volume fractions by innovating extent of constitutive equations has also been addressed. The similar form of the constitutive equation built-up in [6]. Also developed by [5] and confirmed the theory for the particular cases of steady twodimensional shear and elongational flows. Alternative bulk constitutive equation developed by [7] adopting fibre suspension flow alignment assumption.

For the simulation of both planar and axisymmetric contraction and expansion flows [8] has used the idea of [7] adopting semi implicit Taylor Galerken/ Pressure Correction algorithm. The scheme they employed takes wide range of fibre concentration and inertial values without encountering any numerical instability as previously observed limit points of around 12 of [9]. The range of fibre constant reached hundred and beyond, which allows the consideration of dilute to semidilute suspension flows against the constitutive theory derived for dilute suspensions in creeping motion. Including inertia, increased from stokesian flow to inertial flow taking the Reynolds number of over twenty, where fibres lose their impact on flow structure. Successively investigated that how far the creeping flow theory can be extended as inertia begins to take effect. Also provided some plane flow solutions in both rectangular and circular coordinate system, and for axisymmetric expansions they contrast co-linear and orthogonal alignment conditions, and compared against experimental results [10].

For extensional viscosity of suspension of long fibres between dilute and a semi dilute regime the formulae of [2] was improved by [11]. On the rheology of suspension, the motion of suspended particle and liquid, and the influence on each other was identified. A rheological model was developed for the motion of individual fibre in a homogeneous flow field, and the evolution of distribution of the orientation of such fibres [11]. The contribution of the bulk stress was calculated, due to fibres in terms of bulk flow which requires computation of appropriate averages using the orientation function.

For the equations governing the flow of fibre suspension to establish the existence and uniqueness of the solution investigated [12] and focused on the problem in which the presence of fibre is accounted for the inclusion of second order tensor known as orientation tensor, which accounts in the distribution of fibres in the fluid. The use of orientation tensor was first suggested by [13] and subsequently by [14]. The use of orientation tensor as a field variable has the advantage that the behaviour of fibre may be characterised in an averaged way, and in a manner which permits a completely deterministic problem to be treated. The advantage gained was that the orientation tensors are continuum quantities, so the governing equations as well as subsequent analysis and numerical studies may be found on well known approaches [8 and 14].

The flow of fibre suspended in a Newtonian solvent through an axisymmetric expansion and contraction flow [15] investigated and adopted finite element method together with Brownian Configuration Field (BCF) method, originally suggested by [16], which does not need any closure approximations and can obtain good quality results at high volume concentrations of fibres. Also implemented the technique to model the fibre suspension flows with shear induced migration and compared computational results with experimental

data very well. Adopted constitutive models used by [7, 8 and 17] and investigates formation and enhancement of vortex structure in contraction as well as expansion for fibre suspension flows. Effects of different expansion and contraction ratios, volume fraction and aspect ratios of fibres were investigated.

Fibre orientation in a simple moulding process, [18] used hybrid closure approximation for simulation, originally developed by [14]. Hybrid closure approximation is a combination of linear and quadratic approximation, which is exact for random alignment and gives a correct answer for perfectly aligned fibres respectively. The objective of study was to predict short fibre orientation in a liquid polymer flow and their effect on the flow characteristics of suspensions during a mould-filling process by using hybrid closure approximation.

Flow through a periodically constructed tube has an industrial importance and present challenge to numerical researchers, due to its variety of applications and unavailable close form of the problem. This problem is simulated extensively adopting various numerical techniques. Flow through a periodically constricted tube was originally investigated by [19], and subsequently by [20 and 21], using the Finite Difference methods for testing inertial flow of Newtonian fluid and the effect on flow resistance. Later on [22] presented Finite Element predictions for both Newtonian and Non Newtonian fluids using Power Law shear viscosity and extensional viscosity, and demonstrated influence of the inertia and extensional viscosity on flow resistance.

The numerical method used by [21] employed a low order finite difference approximation of the derivatives which was criticised by [20] and presents enough evidence on invalidity and inaccuracy of their results. Recently, several finite element methods have been used to solve this problem by different researchers [22 and 23].

Present study investigates the flow of fibre suspension through a periodically constructed tube. This problem is particularly chosen as suitable test case as it presence both converging and diverging sections and reduce shear and elongational motion at a same time and relatively have simple domain. Two different undulation levels, i.e., thirty percent (30%) and fifty percent (50 %) are selected to investigate the effects of undulation and influence of inertia (Re) on flow structure, fraction factor f, and flow resistance fRe is investigated. The growth of recirculation flow rate (Qv) at different Reynolds number from zero to one thousand, are particularly focused. At both undulation levels, start of recirculation at critical points are realised in present work. For all cases, the fibre constant Fc = 0, 1, 10 and 20 are taken. The numerical simulations utilize a finite element time stepping technique based on a semi implicit Taylor Galerken/pressure correction scheme [22] and solutions are obtained for inertial flows of Newtonian fluids to compare against [11, 21 and 22].

In Section 2, the complete problem is specified and the governing equations and numerical method are described in Section 3. Numerical results and discussions are presented in Section 4 and conclusions are drawn in Section 5.

2. PROBLEM SPECIFICATION

Flow of Fibre suspension through periodically constricted tube is considered as a domain of the interest. As on the assumption that fibre suspension flow is axi-symmetric in circular tube, therefore, the flow is only considered for thin film in upperhalf of undulating

tube, the schematic diagram of domain is shown in Figure1. The radius of the undulating tube wall along the flow axis is given by the following formula:

$$r_w = R\left[1 + \lambda\,Cos\left(\frac{2\pi z}{L}\right)\right]$$

Where R is the average radius of the equivalent straight tube, both λ and L are the dimensionless amplitude of the undulation and wave length respectively. Let (r, z) be coordinates where z-axis is taken as axial direction along the axis in the flow of fibre suspension, while r is along radial direction.

In order to specify the well posed problem the essential initial and mixed Dirichlet and Neumann boundary conditions are taken as follows:

Initial Conditions: Quiescent initial flow condition is imposed for both velocity components such as:

$$v_r(z, 0) = v_z(r, 0) = 0$$

For Momentum Transport Equation the Boundary Conditions adopted are as follows:
1. At solid wall: no-slip $v_r = v_z = 0$.
2. At exit: $v_r = p = 0, v_z =?$.
3. At axis of symmetry: $v_r = 0$ and traction free condition: $\frac{\partial v_z}{\partial r} = 0$.
4. At Inlet: $v_z = v_{\max}\left\{1 - \left(\frac{r}{R}\right)^2\right\}$.

3. GOVERNING SYSTEM OF EQUATIONS

Consider the flow of fibre suspension for Newtonian solvent through PCT governed by the conservation of mass and axisymmetric momentum transport equations in cylindrical polar co-ordinates in the absence of body forces and nondimensional form equations can be presented as:

Continuity equation:

$$\nabla.v = 0.$$

Momentum Equation:

$$\frac{\partial v}{\partial t} = \frac{1}{\text{Re}}\nabla.\left\{2\,D + F_c D :< qq >< qq >\right\} - (v.\nabla)v - \nabla p$$

Where $v \equiv (v_r, v_z)$ is the velocity vector field in r and z directions, p is isotropic fluid pressure and t is time. Whilst, D and $< qq >$ are rate of deformation and second order orientation tensors respectively and is defined as:

$$D = \frac{1}{2}\left[\nabla v + (\nabla v)^\dagger\right] and < qq >= \frac{vv}{|v.v|},$$

Where, F_c is the Fibre constant, defined as:

$$F_c = \phi_{vol}\frac{r_a^2}{\ln(r_a)}$$

While, Re denotes the Reynolds number defined as:

$$\text{Re} = \frac{\rho V R}{\mu_0}$$

The characteristic velocity is V_c, the characteristic length scale is the radius, R, of the straight tube and the characteristic viscosity μ_c is the zero shear-rate viscosity. Appropriate scaling in each variable takes the form.

4. Numerical Scheme

For the fibre suspension the numerical simulations utilize a finite element time stepping technique based on a semi implicit Taylor Galerken/pressure correction scheme [24]. This scheme was initially developed for flow Newtonian fluid and later on extended its range to cover complex flows of Viscoelastic fluids by incorporating Petrove-Galerken streamline up-winding in the time stepping framework [8]. To describe this method, summary is given here for completeness. This technique contains time discretization in Taylor series combined with predicator-corrector scheme. To find the second order time derivatives, two steps LaxWendroff approach have been employed. These schemes show an extensive development in accurateness and steadiness with respect to both finite deference and $Euler - Galerken$ finite element Schemes [8]. $Pressure - correction$ method assures second order accuracy and stability through linearised energy analysis, and when it combined with predicator- corrector Taylor Galerken technique [8-22], the base for presenting numerical scheme adopted in this research work is provided to obtain the time independent results.

The numerical simulations are conducted in multistage form. In the momentum transport equation the presence of nondimensional additional diffusion term on the R.H.S that represents the presence of fibre additive in cylindrical frame of reference is given at half time step in first part of stage one. Initially, at stage one solution is obtained at half time step. In second part of stage one, an intermediate non-solenoidal velocity field has been calculated. At stage two Pressure difference is calculated by solving the Poisson equation. The Crank-Nicolson scheme is adopted to get the second order level of accuracy, while solenoidal velocity has been obtained in third and final stage. Both stages one and three are governed by the augmented mass matrices, and are iteratively solved very efficiently in a handful of iteration by Jacoby Method which avoids the system matrix assembly that is helpful component for solution process. At stage two we adopted direct Choleski solution method, because the pressure matrix is symmetric and is positive definite with bounded structure. Solving the problem, equations are discritised through standard Galerken weighted residual method and mixed velocity pressure formulation is used for finite element approximation and triangular element chosen here for domain. Both piecewise linear and quadratic functions for velocity and pressure are employed.

Stage1(a): Given $\left(v^n,\ p^n\right)$, find $v^{n+\frac{1}{2}}$ such that

$$\frac{2}{\Delta t}\left(v^{n+\frac{1}{2}} - v^n\ ,v\right) + \frac{1}{2\,\mathrm{Re}}\left(\nabla\left(v^{n+\frac{1}{2}} - v^n\right),\nabla v\right)$$
$$= \left(p^n - \frac{1}{\mathrm{Re}}\nabla v^n + F_c\left(D : \frac{vv}{|v.v|}\frac{vv}{|v.v|}\right)^n,\nabla v\right) - \left(\left(\left(v.\nabla\right)v\right)^n,v\right)$$

Stage1(b): Given v^n, $v^{n+\frac{1}{2}}$, p^n, find v^* such that:

$$\frac{1}{\Delta t}\left(v^* - v^n\right), v \quad + \frac{1}{2\,\mathrm{Re}}\left(\nabla\left(v^* - v^n\right), \nabla v\right)$$

$$= \quad p^n - \frac{1}{\mathrm{Re}}\nabla v^n + F_c \quad D : \frac{vv}{|v.v|}\frac{vv}{|v.v|}^{n+\frac{1}{2}}, \nabla v\right) - \quad \left((v.\nabla)\,v\right)^{n+\frac{1}{2}}, v$$

Stage2: Given v^* and p^n, find $p^{n+1} - p^n$ such that:

$$\theta\,\nabla\quad p^{n+1} - p^n\quad, \nabla q\ = \frac{-1}{\Delta t}\left(\nabla v^*, q\right)$$

Stage3: Given v^* and $p^{n+1} - p^n$, find v^{n+1} such that:

$$\frac{1}{\Delta t}\quad v^{n+1} - v^*\quad, v\ = \ \theta\quad p^{n+1} - p^n\quad, \nabla v$$

5. Numerical Results and Discussions

Numerical computations are carried out for flow of fibre suspension through two different undulation levels of the domain, to investigate the effect of amplitude of undulation, influence of inertia on flow structure in the form of streamlines and pressure isobars. Start of recirculation has been identified at different critical limit points of Reynolds number values. Fraction factor, flow resistance and vortex enhancement at different Reynolds number with increasing fibre constants are also investigated. Numerical solutions have been obtained for inertial flows of Newtonian fluids to compare against experimental data, investigated in the literature [19] and other numerical results produced [21-22]. For each undulation level, streamlines projections are plotted at constant incremental values in two main parts, core flow and recirculation area. Seven contours are chosen in the main core flow region, for thirty percent undulation, that are, 0.001, 0.01, 0.05 0.1.0.15, 0.2 and 0.24 (Q/2) on the line of symmetry of non dimensional values of stream functions while in the fifty percent undulation, again seven contours are chosen to describe the core flow, which are, 0.001, 0.02, 0.04, 0.06, 0.08, 0.1 and 0.12. In all the undulation levels, in the region where the vortex development occurs, ψ_{min} is employed to represent the slower regions. All contours in a recirculation region represented from the centre of the vortex i.e., innermost contour to the periphery ψ_{per} of the vortex i.e., outermost contour. Two finite element meshes are adopted for computation to validate the algorithm, which has been used in this investigation.

5.1. **Effects of Inertia on Flow Structure:** The inertial flow of Newtonian fluid through all selected levels of periodically constricted tube is analysed to understand the effects of inertia on the flow structure. Streamline projections are described here with increasing the values of Reynolds number (Re). In Figure 4 and Table 2, from computed data it is clear that in thirty percent undulation no vortex is observed at low Reynolds number up to 40, and streamlines representing main core flows are almost attached with undulation wall. The development of vortex starts approximately at Re = 41 close to undulation upstream wall. As Reynolds number increases vortex centre moving from upstream to the centre of the undulation and grow larger. This process of the development of vortex as in left side of the Figure: 5, grows more and strengthens, and the centre of vortex moves further to the centre and occupy whole undulation. Whilst, in fifty percent undulation, recirculation develops at low Reynolds number Re= 28 and similar phenomenon of vortex enhancement occurs. In right of the Figure: 5, recirculation increased as inertia increased at high Reynolds number

and size of vortex is enhanced as level of undulation increased and observed at the centre of undulation. At Reynolds number 500, core flows becomes almost straight, vortex enhanced more, and centre of the vortex shifted towards the downstream, while by increasing the inertia at Re=1000, it is observed that centre of the larger recirculation region moves further to downstream and instability is observed in the shape of the vortex, the main core flows observed very much straight. In table: 1, the numerical results of present study are compared against the experimental results of [19], and numerical results of [21 and 22].

For the flow of pure Newtonian case at Re = 500, pressure drop is demonstrated in figure- 6 within periodically constricted tube at both undulation levels of 30% and 50%. Pressure contours in thirty percent undulation are plotted from 5.5126e-023 to 0.16003, whilst for fifty percent the contours are plotted from 7.1593e-023 to 0.24885. The figure clearly illustrates that maximum pressure drop moves from inlet in the vicinity of converged wall to outlet in the neighbourhood of diverging wall. Therefore, non-linear inertial influence on the friction factor (fRe) as function of rise in Reynolds number. However, in recirculation region non linearity is not observed. It is extremely complex flow phenomenon, even at low inertial values flow resistance is also low where recirculation region is not developed. On the contrary, the value of friction factor increased than the corresponding Stokian value. The predicated numerical results in this study are investigated at three different maximum velocities. Due to nonavailability of precise information on flowrate solution are not in fully agreement with the experimental results of [19] and numerical predictions of [21 and 22].

TABLE 1. Comparison Table for flow risistance (fRe) of Newtonian fluid

Re	Lahbabi and Chang	Pilitsis, et al.	Baloch and Memon	Present Study		
				$(V_{max} = 2)$ $\psi_{max} = 0.245$	V_{max} =1.299224	V_{max} =1.297959
00	26.4	26.4483	26.382	26.674	26.724	26.700
12	27.1	27.179	26.913	26.891	26.815	26.800
22	28.5	28.5536	27.889	27.346	27.238	27.100
51	31.7	31.7484	30.643	32.525	29.203	30.600
63	32.6	32.6758	32.601	34.468	31.520	31.500
73	33.4	33.4488	33.150	35.754	33.117	33.100
132	36.7	36.5264	35.961	40.458	38.928	37.100
264	39.7	40.2446	39.964	45.519	42.401	42.400
400	40.6	42.3491	41.966	48.655	45.440	45.400
600	40.9	44.0371	43.103	52.162	48.521	48.500
783	41.8	45.5828	44.058	54.880	50.815	50.800

5.2. **Influence of Suspended Fibres on Flow Structure:** The influence of suspended fibres in a Newtonian solvent under simple shear flow through PCT is analysed with increasing Reynolds number and different fibre constants (F_C). Colinear fibre constitutive model is adopted along with quadratic closure approximation to investigate the numerical results by setting the levels of fibre constant as $F_C = 1, 10$, and 20. From all values of

fibre constants at two undulation levels, it is observed that the presence of suspended fibres in Newtonian solvent flow has noticeable influence on flow structure over pure flow of Newtonian fluid. For each value of fibre constant, inertia is taken from Stokian to high Reynolds number up to order of O(3) using the semi implicit algorithm, so called, TaylorGalerken/pressure correction scheme. The steadystate numerical predictions are sought out for both undulation levels to analyse the shape and flow rate (Q_V) as a function of both F_C and Re in the recirculation region, as applied by [7, 8, and 9].

In thirty percent undulation with F_C=1, up to low Reynolds Number of Re=37, no recirculation has been observed and main core flow occupy whole undulation area. Recirculation starts at Re=38, very close to the centre of undulation and attached with wall and demonstrated in left side of Figure 7. The limiting value of inertia decreases further as the value of fibre constant increase where recirculation starts. With F_C=10, it starts at Re=23, whilst, at F_C=20 it develops at very low value of inertia of Re = 06, this limit point more decreases as fibre constants increases. At high level of Reynolds number (Re=100), with fibre constant $F_C = 1$, and $F_C = 20$, the influence of fibre and effects of inertia on vortex enhancement similar to those reported above in pure Newtonian flow cases with slightly change in the size of vortex as by introducing the fibre the size of vortex decreases. With other high Reynolds numbers Re = 500 and Re = 1000, the size of vortex inhibits and occupy the whole undulation area but the centre of recirculation in pure Newtonian case witnessed moving towards downstream. Whilst in the presence of fibre, the development of recirculation region is observed close to the centre of undulation.

In Table 2 and in right side of Figure 7,critical limit points of Reynolds number, where recirculation starts, are presented for fifty percent undulation with chosen fibre constants. Recirculation realised at low Re = 23 with fibre constants $F_C = 01$, as fibre constant depart from low value to $F_C = 10$ and $F_C = 20$, this embryo vortex develops further and reduce the level of inertia i.e., Re = 03 and Re = 02 respectively. In Figure 9, beyond the critical Reynolds numbers Re= 100, 500, 1000 are presented, the shape and size of vortex observed entirely different as observed in the pure Newtonian flow cases. With the introduction of fibre constant, the centre of vortex predicted almost at the centre of undulation, whilst in pure Newtonian flow cases it shifts from centre to downstream region. Furthermore, with fibre constant $F_C = 10$, in Figure 10, the core flow observed unstable and size of vortex also reduced similar as in thirty percent undulation at the same level of fibre constant.

TABLE 2.   Critical Reynolds Number at Different Undulation Levels.

Level of Undulation	Fibre Constant (F_C)			
	$F_c = 00$	F_c=01	F_c=10	F_c=20
30 Percent	41.00	38.00	23.00	06.00
50 Percent	28.00	23.00	03.00	02.00

5.3. **Impact of undulation on Flow Structure:** The impact of amplitude of undulation on flow structure for both pure Newtonian and fibre suspended in Newtonian solvent is analysed in the form of flow structure, vortex enhancement and fraction factor. Streamlines represents flow structure and recirculation flow rate demonstrate the vortex growth

in the form of size and intensity. The streamline projections show the distinct effects on flow field at both the levels of undulation by introducing the fibre level in the Newtonian solvent. The behaviour of flow analysed at various Reynolds number. It is observed that development of recirculation starts when value of inertia decreased as level of undulation increase.

For all fibre constants, the flow through both undulations the graph of the vortex intensity is plotted in Figure 12 from Reynolds number 1 to 1000. Left side of the Figure 12 represents the vortex intensity for thirty percent undulation while, in right of figure12 it is plotted for fifty percent undulation.

TABLE 3. Friction Factor (fRe) on both undulation levels with increasing Reynolds Number.

| | Level of undulation | | | | | | | |
| | 30 Percent | | | | 50 Percent | | | |
Re	F_c=00	F_c=01	F_c=10	F_c=20	F_c = 00	F_c=01	F_c=10	F_c=20
1	1.5708	1.5708	1.5708	1.5708	1.5708	1.5708	1.5708	1.5708
50	2.1166	2.0621	3.8154	6.5591	2.0628	2.2155	4.5882	5.7914
100	2.3677	2.6137	8.3008	13.623	2.6869	2.9534	7.1413	12.3377
500	3.0583	4.711	26.029	72.693	3.7660	5.2813	25.5306	58.7391
1000	7.6446	7.6644	117.027	170.11	4.2850	8.7592	75.7636	123.3516

Another primary interest of the present investigation is to analyse the flow resistance (friction factor) as the function of Reynolds number and relative pressure difference, defined as:

$$f = \frac{\pi^2 \Delta p R^5}{\rho L Q^2}$$

Where R is the average radius, L is the amplitude wave length, Q is the flow rate, ρ is the fluid density and p is relative pressure difference and can be defined as:

$$\Delta p = \frac{\text{Re} \cdot \|p_{\max} - p_{\min}\|_{\text{Re}>1}}{\|p_{\max}\|_{\text{Re}=1}}$$

In Figure 13 the computed results of friction factor are graphically illustrated for both undulation levels. The values of inertia are taken from zero to Re = 1000. Figure clearly indicates that as inertia increase friction factor increase nonlinearly in an exponential fashion. With the introduction of fibres the flow resistance increase and this rapidly increase as fibre constant increase. Calculated data of these phenomena is illustrated in Table 3.

The empirical relationships for friction factor are developed based on computed solutions against the five different Reynolds number and all chosen fibre constants for both the levels of undulation are calculated and presented in Figure 14 and tabulated in Table 4.

TABLE 4. Empirical Equations of thirty and fifty percent undulation
with increasing fibre Constant.

		Empirical Equations	
S.No	Fibre Level	30 Percent Undulation	50 Percent Undulation
1	00	$X=(0.0056)$Re$+1.51540$	$X=(0.0025)$Re$+2.0488$
2	01	$X=(0.0059)$Re$+1.77620$	$X=(0.0069)$Re$+1.8777$
3	10	$X=(0.1106)$Re-5.171520	$X=(0.07198)$Re-0.8492
4	20	$X=(0.1684)$Re-2.694520	$X=(0.1221)$Re$+0.0407$

6. CONCLUSIONS

Adopting Taylor Galerken/Pressure Correction Scheme the steady state numerical solutions are obtained. The comparison is made between computed solutions against other numerical predictions and experimental results. The influence of inertia (Re) on flow structure, fraction factor f and flow resistance fRe is investigated. The vortex enhancement (Qv) at different Reynolds number is particularly focused. At different undulation levels, start of recirculation, i.e. Critical Limit Points of Reynolds number is realised.

REFERENCES

[1] T. Abdul-Karem, D.M. Binding and M. Sindelar, *Contraction and expansion flows of non-Newtonian fluids*, to appear in J. Non-Newtonian Fluid Mech. **4**, No. 2 (1993) 109-116.

[2] S.G. Advani and C.L. Tucker, *The use of tensors to describe and predict fibre orientation in short fibre composites*, J. Rheol. **31**, (1990) 751-784.

[3] A. Baloch and M.F. Webster, *A Computer Simulation of Complex Flows of Fibre Suspensions*, J. Computers and Fluids, **24**, No. 2 (1995) 135-151.

[4] A. Baloch, P. Townsend and M.F. Webster, *On the Simulation of Highly Elastic Complex Flows*, J. non-Newtonian Fluid Mech. **59**, No. 2-3 (1995) 111-128. doi:10.1016/0377-0257(95)01369-7

[5] A. Baloch and A.S. Memon *Simulation of corrugated tube flow of non Newtonian fluids*, MUETJET, **26**, No. 1 (2007) 19-32.

[6] G.K. Betchelor, *The stress system in a suspension of force-free particles*, J. Fluid Mechanics, **41**, No. 3 (1970) 545-570.

[7] K. Chiba, K. Nakamura and D.V. Boger, *A numerical solution for the flow of dilute fibre suspension through an axisymmetric contraction*, J. Non-Newtonian Fluid Mech. **35**, (1990) 1-14.

[8] R.G. Cox and H. Brenner, *The rheology of a suspension of a particle in a Newtonian fluid*, J. Chem. Eng. Sci. **26**, (1971) 65-93.

[9] M.J. Crochet, V. Delvaux and J.M. Marchal, *On the Convergence of Streamline-Upwind Mixed Finite Element*, International Journal of Non-Newtonian Fluid Mechanics, **34**, (1990) 261-268.

[10] S.M. Dinh and R.C. Armstrong, *A Theological equation of state for semi concentrated fibre suspensions*, J. Rheol. **28**, No. 3 (1984) 207-227.

[11] J.G. Evans, *The effects of the non-Newtonian properties of a suspension of rodlike particles on flow fields*, In: Theoretical Rheology, Eds. Hutton, J.F., Pearson, J.R.A., and Waiters, K., Applied Science, London, (1975) 224-232.

[12] X.J. Fan, N. Phan-Thein and R. Zheng, *Simulation of fibre suspension flow with shear induced migration*. J. Non-Newt. Fluid Mech. **90**, (2000) 47-63.

[13] G.P. Galdi and B.D. Reddy, *Well-posedness of the problem of fibre suspension flows*, J. Non-Newtonian Fluid Mech. **83**, (1999) 205-230.

[14] G.L. Hand, *A theory of anisotropic fluids*, Journal of Fluid Mechanics, **13**, (1962) 33-46.

[15] G.B. Jeffery, *The union of ellipsoidal particles immersed in a viscous fluid*, Proc. R, Soc, A 102, 161, 1922.

[16] A. Lahbabi and H.C. Chang, *Flow in periodically Constricted Tubes: Transition to Inertial and Unsteady Flows*, J. Chemical Engineering Society, **41**, (1986) 2487-2505.
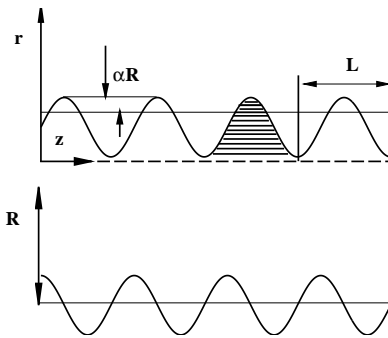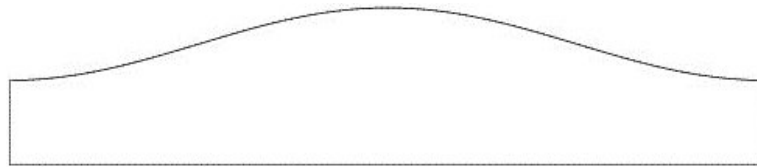
FIGURE 1. Domain for flow through PCT.

FIGURE 2. Computational domain of concentricted tube flow.

[17] L.G. Leal and E.J. Hinch, *Theoretical studies of a suspension of rigid particles affected by Brownian couples*, Rheol. Acta. **12**, (1973) 127-132.

[18] G.G. Lipscomb, M.M. Denn, D.U. Hur, and D.V. Boger, *The flow of fibre suspension in complex geometries*, J. Non-Newtonian Fluid Mech. **26**, (1988) 297-325.

[19] Z. Lu, B.C. Khoo, H.S. Dou, N.Phan-Thein and K.S.Yeo, *Numerical Simulation of Fibre Suspension Flow through an Axisymmetric Contraction and Expansion Passages by Brownian Configuration Field Method*, J. Chemical engineering science, **61**, (2006) 4998-5009.

[20] A.N. Oumer, M.S. Ali and O.B. Mamat, *Numerical Simulation of Fibre Orientation in Simple Injection Moulding Processes* IJMME **9**, No. 9 (2010) 361-367.

[21] C.J.S. Petrie, *The Rheology of Fibre Suspensions, J. Non-Newtonian Fluid Mechanics*, **87**, (1999) 369-402.

[22] N. Phan-Thein and A.L. Graham, *A new constitutive model for fibre suspensions: flow past a sphere*, J. Rheol. Acta, **30**, (1991) 44-57.

[23] S. Pilitsis, A. Souvaliotis and A.N. Beris, *Viscoelastic Flow in a periodically constricted tube: The combined effect of inertia, shear thinning, and elasticity* J. Rheology, **35**, No. 4 (1991) 605-646.

[24] Q.H. Zhang and J.L. Zhong, *Orientation distribution and rheological properties of fibre suspensions flowing through curved expansion and rotating ducts*, 9th international conference on Hydrodynamics, 2010.
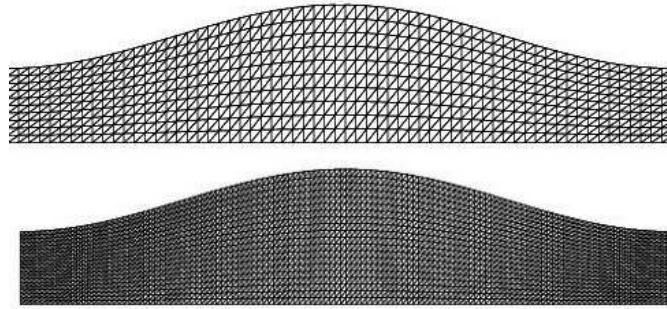
FIGURE 3. Finite element meshes of concentricted tube flow ((left) Coars Mesh, (right) Refined Mesh).
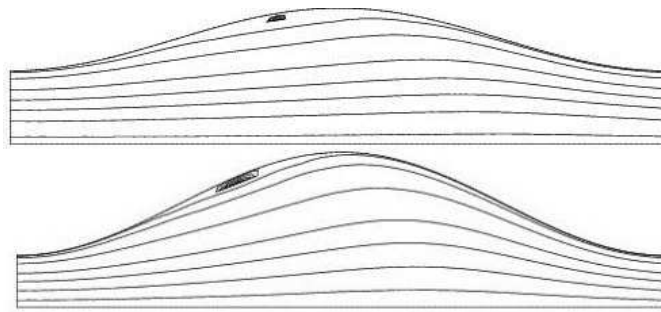
FIGURE 4. Streamlines for both 30% and 50% undulation at critical Reynolds numbers.
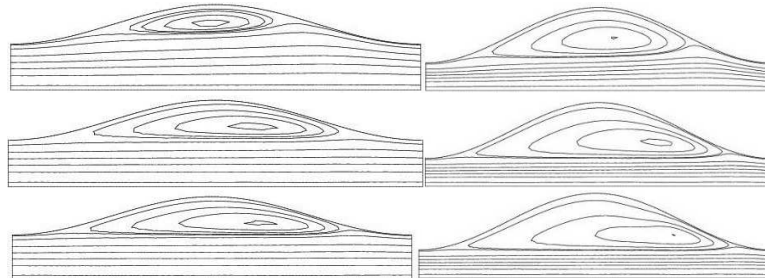

FIGURE 5. Streamlines for both 30% (left) and 50% (right) undulation with increasing Reynolds Numbers (=100, 500 and 1000.)
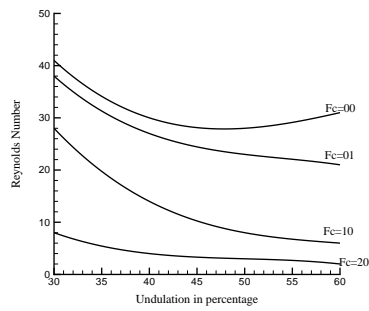
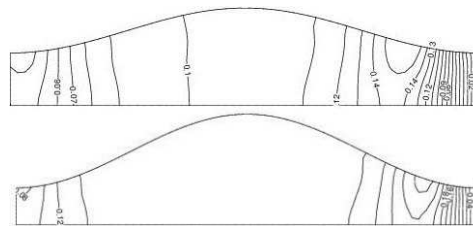FIGURE 6. Critical Reynolds Number at Different Undulation Levels.

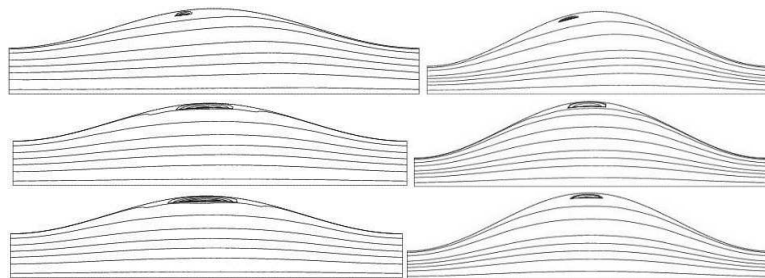FIGURE 7. Graph of Pressure drop in both 30% and 50% undulation at Re= 500.

FIGURE 8. Streamlines for 30% (left) and 50% (right) undulation at critical Reynolds Numbers (Fc=01, 10 and 20).
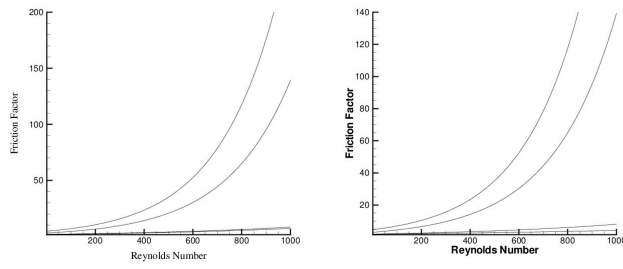
FIGURE 9. Vortex Intensity at 30% (left) and 30% (right) undulations with increasing fibre constant and Reynolds numbers.
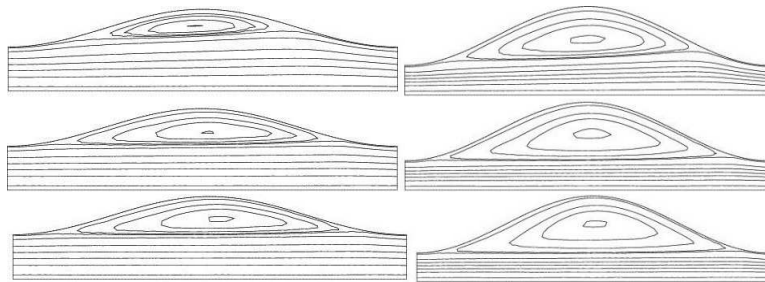
FIGURE 10. Streamlines for 30% (left) and 50% (right) undulation with increasing Reynolds Numbers.
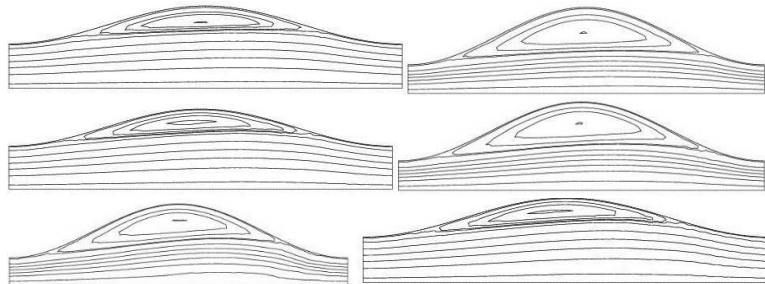
FIGURE 11. Streamlines for 30% (left) and 50% (right) undulation with increasing Reynolds Numbers.
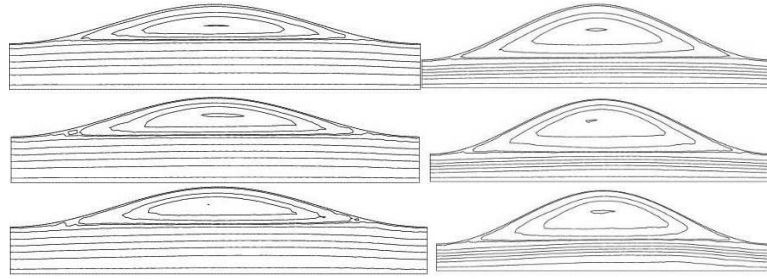
FIGURE 12. Streamlines for 30% (left) and 50% (right) undulation with increasing Reynolds Numbers.
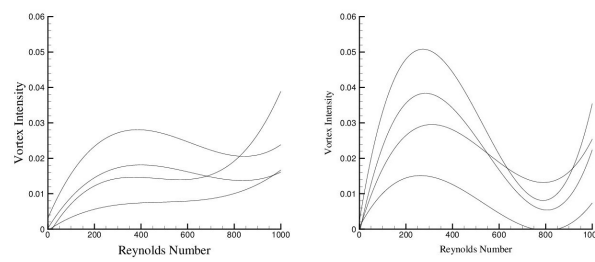

FIGURE 13. Vortex Intensity at 30% (left) and 30% (right) undulations with increasing fibre constant and Reynolds numbers.
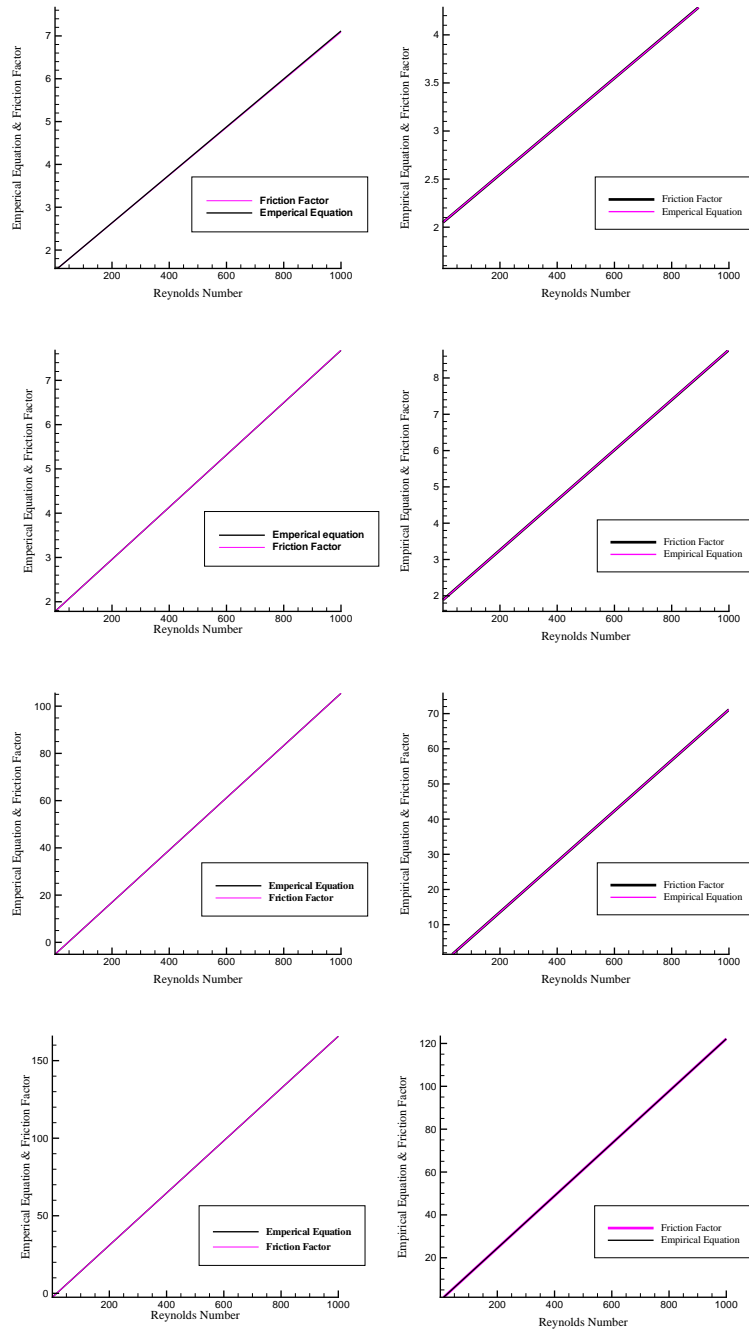
FIGURE 14. Graph of the Empirical equations at 30% (left) and 50% undulations with increasing fibre constant.